Oecologia (2013) 173:625–635
DOI 10.1007/s00442-013-2650-7

PHYSIOLOGICAL ECOLOGY - ORIGINAL RESEARCH

Diverging drought-tolerance strategies explain tree species distribution along a fog-dependent moisture gradient in a temperate rain forest

Beatriz Salgado Negret · Fernanda Pérez · Lars Markesteijn · Mylthon Jiménez Castillo · Juan J. Armesto

Received: 1 August 2012 / Accepted: 22 March 2013 / Published online: 11 April 2013

Abstract The study of functional traits and physiological mechanisms determining species' drought tolerance is important for the prediction of their responses to climatic change. Fog-dependent forest patches in semiarid regions are a good study system with which to gain an understanding of species' responses to increasing aridity and patch fragmentation. Here we measured leaf and hydraulic traits for three dominant species with contrasting distributions within patches in relict, fog-dependent forests in semiarid Chile. In addition, we assessed pressure–volume curve parameters in trees growing at a dry leeward edge and wet patch core. We predicted species would display contrasting suites of traits according to local water availability: from one end favoring water conservation and reducing cavitation risk, and from the opposite end favoring photosynthetic and hydraulic efficiency. Consistent with our hypothesis, we identified a continuum of water use strategies explaining species distribution along a small-scale moisture gradient. *Drimys winteri*, a tree restricted to the humid core, showed traits allowing efficient water transport and high carbon gain; in contrast, *Myrceugenia correifolia*, a tree that occurs in the drier patch edges, exhibited traits promoting water conservation and lower gas exchange rates, as well low water potential at turgor loss point. The most widespread species, *Aextoxicon punctatum*, showed intermediate trait values. Osmotic compensatory mechanism was detected in *M. correifolia*, but not in *A. punctatum*. We show that partitioning of the pronounced soil moisture gradients from patch cores to leeward edges among tree species is driven by differential drought tolerance. Such differences indicate that trees have contrasting abilities to cope with future reductions in soil moisture.

Keywords Climate change · Fog-dependent forest · Local water gradient · Species distribution · Plant hydraulic traits

Communicated by Gerardo Avalos.

B. S. Negret · F. Pérez · J. J. Armesto
Departamento de Ecología, Pontificia Universidad Católica de Chile, Casilla 114-D, Santiago, Chile

B. S. Negret (✉) · F. Pérez · J. J. Armesto
Instituto de Ecología y Biodiversidad, Casilla 653, Santiago, Chile
e-mail: besalgad@uc.cl

L. Markesteijn
Departamento de Biogeografía y Cambio Global, Museo Nacional de Ciencias Naturales, Consejo Superior de Investigaciones Científicas (CSIC), Serrano 115 dpdo, 28006, Madrid, Spain

M. J. Castillo
Instituto de Ciencias Ambientales y Evolutivas, Universidad Austral de Chile, Casilla 567, Valdivia, Chile

M. J. Castillo
Jardín Botánico Universidad Austral de Chile, Facultad de Ciencias, Universidad Austral de Chile, Casilla 567, Valdivia, Chile

Introduction

Water availability is a major factor influencing species distribution in forest communities across large-scale rainfall gradients as well as small-scale topographic gradients (Gentry 1988; Wright 1992; Condit 1998; Bongers et al. 1999; Pyke et al. 2001; Condit et al. 2002; Engelbrecht et al. 2007). A species' distribution may be explained by functional trait divergence associated with performance

under particular conditions of soil humidity (Poorter 2007; Markesteijn et al. 2011a; Sterck et al. 2011). Understanding the bases of such differentiation among forest trees may be critical for predicting the ecological consequences of the future alteration of soil moisture gradients due to climate change.

Fog-dependent forests, found in semiarid regions of the world (Hildebrandt and Eltahir 2006; del-Val et al. 2006; Katata et al. 2010), are thought to be relicts from past periods when conditions were more humid, and thus these ecosystems might be especially sensitive to current changes in fog water supply. Alterations in fog frequency and intensity are predicted to occur due to changes in sea-surface temperature and the height of the temperature inversion layer (Cereceda et al. 2002), loss of forest patch area and fragmentation, or changes in forest structure affecting fog capture (Hildebrandt and Eltahir 2006). In these patchy forests, fog interception by plants is the primary or even the only source of water during most of the year (Dawson 1998; del-Val et al. 2006; Ewing et al. 2009). The fog interception by trees creates pronounced water and nutrient gradients from windward to leeward edges in forest patches (Weathers et al. 2000; del-Val et al. 2006; Ewing et al. 2009), with strong contrasts over short distances, depending on wind direction (Ewing et al. 2009). Studying tree species' responses to soil moisture variation at short spatial scales, due to topographic and/or patch fragmentation gradients in these fog-dependent ecosystems, allows us to address questions about the critical conditions for sustaining tree species under increasing drought stress due to changing climate.

Our study site, the Fray Jorge forest in central Chile, is a striking example of such a fog-dependent ecosystem, where the strong water (and possibly nutrient) gradients inside the isolated forest patches affect the distribution and regeneration dynamics of tree species (del-Val et al. 2006). The patches are dominated by species characteristic of temperate and Mediterranean forests in Chile: *Aextoxicon punctatum* (in the monotypic family Aextoxicaceae) is found in all-size patches but it is more frequent in humid windward edges, directly facing the incoming fog; *Drimys winteri* (Winteraceae) tends to be aggregated in the interior of the largest forest patches and is not found in small patches; finally, *Myrceugenia correifolia* (Myrtaceae) is more common along the edges of small patches, including the drier leeward edge (del-Val et al. 2006; Gutiérrez et al. 2008). Such contrasting distribution patterns, and the pronounced short-distance, environmental gradients related to moisture supply by fog, offer a great opportunity to investigate the physiological mechanisms that explain a tree species' ability to respond to abrupt and pronounced changes in climate due to global warming.

Convergence in leaf traits reducing water loss by transpiration, as well as hydraulic traits favoring safety at the expense of hydraulic efficiency, has been reported for plants that are periodically exposed to severe water deficit (Mitchell et al. 2008; Markesteijn et al. 2011a, b). Such plants usually show narrower and shorter vessels with small pit pores, which are more resistant to drought-induced cavitation, but at the same time have an increased flow resistance and a lower hydraulic efficiency (Hacke et al. 2001; Choat et al. 2005; Mitchell et al. 2008; Markesteijn et al. 2011a, b), affecting leaf water supply. The capacity to maintain leaf turgor in response to decreasing soil moisture availability is also an important mechanism that favors drought tolerance (Kozlowski and Pallardy 2002; Baltzer et al. 2008; Kursar et al. 2009; Bartlett et al. 2012). Water potential at loss turgor point (π_{tlp}) is a critical physiological determinant of a plant's tolerance to water stress (Bartlett et al. 2012). Plants can reduce π_{tlp} by accumulating osmotically active compounds in the cells (osmotic adjustment) or by increased cell wall flexibility (bulk modulus of elasticity; ε). However, recently Bartlett et al. 2012) showed no direct role for ε in driving differences in π_{tlp} across species, instead, elastic adjustments acted to maintain relative water content at turgor loss point (RWC_{tlp}) despite very negative water potentials at full turgor (π_0) and π_{tlp}.

Here, we measured leaf and hydraulic traits of the three main tree species occurring in fog-inundated rain forest patches of Fray Jorge (semiarid Chile), which show contrasting distribution patterns along the soil moisture gradient produced by fog influx. We also compared pressure–volume curve traits of individuals growing at windward and leeward edges of forest patches.

Specifically, we addressed the following questions:

1. How does the variation in functional traits related to drought tolerance explain species distribution along small-scale moisture gradients?
2. What mechanisms allow individuals growing along the drier leeward edges to cope with reduced water availability (such as osmotic adjustment or increased cell elasticity) in comparison with conspecific individuals growing in wetter patch core habitats?

We expect that species growing in small patches and leeward patch edges would display a suite of leaf traits favoring water conservation [such as reduced stomatal conductance (g_s)] and a suite of hydraulic traits reducing cavitation risk (such as narrow vessels), at the expense of photosynthesis and hydraulic efficiency. We also predict that individuals growing at the leeward patch edge would have pressure–volume traits values favoring drought tolerance (such as lower π_{tlp} and π_0) in comparison with conspecific individuals growing in the wetter patch core.

Tree species occurring in the fog forest of Fray Jorge are exposed to increased aridity due to climatic changes over

an extended period of time (Villagrán et al. 2004; Gutiérrez et al. 2008), and face seasonal changes in fog influx that drive pronounced moisture gradients within patches (del-Val et al. 2006). This study aims to reveal some of the basic mechanisms underlying the relative success of these species to coexist given past and current variations in moisture availability. Here, we will further discuss results in the light of the possible consequences of future climate change and its effects on species' distribution and coexistence.

Materials and methods

Study site and species

Fray Jorge National Park (30°40′S. 71°30′W) comprises the northernmost patches of Chilean temperate rainforests, dominated by broad-leaved evergreen tree species, which exhibit remarkable floristic affinities with temperate forests located some 1,000 km to the south (Villagrán et al. 2004). The area contains a mosaic of about 180 forest patches ranging in size from 0.1 to 36 ha, located on the summits of coastal mountains at an elevation of 450–660 m, surrounded by a matrix of semiarid scrub vegetation (Barbosa et al. 2010). The regional climate is Mediterranean-arid with a mean annual rainfall of 147 mm concentrated during the cool winter months from May to August and a mean annual temperature of 13.6 °C (López-Cortés and López 2004). Fog is a prominent and constant feature of the landscape above 400 m elevation, especially during spring and summer months, when fragments can receive an additional input of at least 200 mm of cloud water annually via throughfall and stemflow (del-Val et al. 2006).

A large 36-ha patch was selected for this study because it was the only one where all three focal tree species coexist. Additional details on the structure and physical gradients of patches are given by Barbosa et al. (2010). The forest patch studied was located at an altitude of 635 m, with average air temperatures inside the patch varying from 9.2 °C in spring (October–December) to 13.3 °C in winter (July–September) and relative air humidity varying between 83.6 % in winter and 99.6 % in spring-summer.

The forest canopy is dominated by *A. punctatum* (Aextoxicaceae), with juveniles occurring more frequently along the edge directly receiving fog influx (windward), and adults throughout the patch; the canopy is co-dominated by *D. winteri* (Winteraceae), which tends to aggregate inside the patch. *M. correifolia* (Myrtaceae) is occasionally represented in the canopy of the forest patch (0.3 % basal area) but it is confined to the drier leeward edge (Gutiérrez et al. 2008). Volumetric soil moisture varies substantially in both small and large patches. Leeward edges are drier than the other two microhabitats, while soil moisture at the windward edges is comparable with that at the patch core (25 measurements per zone in *A. punctatum* individuals): small patches—windward, 10.43 ± 1.01 %; core, 12.13 ± 1.12 %; leeward, 5.02 ± 0.49 %; large patches—windward, 9.25 ± 0.62 %; core, 14.59 ± 0.72 %; leeward, 4.72 ± 0.30 %) (B. Salgado-Negret, unpublished data). Volumetric soil moisture for our species, measured at 20 cm depth, varied accordingly across sites occupied by the different tree species (30 measurements per species): *D. winteri* (22.9 ± 2.66 %), *A. punctatum* (13.4 ± 1.7 %) and *M. correifolia* (5.3 ± 0.53 %) ($P < 0.0001$; $F = 23.01$; $df = 2$) (B. Salgado-Negret, unpublished data).

The three species have a different phytoclimatic distribution in Chile: *A. punctatum* is a tree species endemic to western South America and it is broadly distributed in coastal forests from 30 to 43°S; *D. winteri* is distributed from Fray Jorge and central Chile to subantarctic forest in Tierra del Fuego at 55°S (Villagrán et al. 2004). Finally, *M. correifolia* is restricted to central Chile with a Mediterranean climate subjected to a cool rainy winter and a summer drought period of 2–3 months (Di Castri and Hajek 1976).

Leaf traits

We measured leaf traits for six individuals (diameter at breast height >10 cm) of each tree species using mature, fully expanded leaves without herbivore damage. All measurements were done on the same six individuals. CO_2 assimilation curves were constructed using the CO_2 reference concentration of 380 p.p.m., 50 % relative humidity, and a temperature of 25 °C. Photosynthesis (A_{max}) and g_s were measured in *M. correifolia*, *A. punctatum* and *D. winteri* at 700, 500 and 700 μmol m^{-2} s^{-1}, respectively, with an open portable photosynthesis system (CIRAS-2 CRS068; PP Systems, Amesbury, USA) equipped with a light-emitting diode. Measurements were conducted between 1000 and 1300 hours. After measurements of gas exchange, leaves were cut and leaf water potentials (ψ) at midday were measured (ψ_{MD}; MPa) using a pressure chamber (Scholander-type, model 1000 PMS). We also measured predawn ψ (ψ_{PD}; MPa) between 0500 and 0700 hours for the same six individuals per species.

After measurement, leaves were scanned (EPSON Stylus TX200) and analyzed using ImageJ software (http://imagej.nih.gov/ij/) to determine leaf area (LA). Finally, leaves were dried for 48 h at 65 °C to obtain leaf dry mass (g) and calculate leaf mass per area (LMA; g cm^{-2}) (Cornelissen et al. 2003).

Pressure–volume curves

Pressure–volume curves were constructed for six individuals per species. One shoot was cut from each individual and the shoots were hydrated with distilled water in plastic bags to bring leaves to full turgor. Tissue rehydration is necessary to ensure that all samples are near saturation, thus allowing for construction of the entire moisture-release curve (Baltzer et al. 2008). After 24 h of rehydration, we constructed pressure–volume curves following the Sack and Pasquet-Kok protocol (www.prometheuswiki.com). Water potentials of the leaves were measured with a Scholander-type pressure chamber (PMS, model 1000) and the tissue was weighed immediately after measurement. The tissue was dehydrated slightly at room temperature, before re-weighing the leaf mass and re-measuring the water potential. This process was repeated until the tissue reached constant mass. When there was no further decrease in mass, leaves were dried for 48 h at 80 °C to determine dry mass. The following traits were estimated from the pressure–volume curves: solute potential at full turgor (π_0; MPa), solute potential at turgor loss point (π_{tlp}; MPa), RWC_{tlp} (%), and ε (MPa).

Hydraulic traits

Maximum vessel length

One branch (2.5–10 mm diameter) was cut from the outer crown of each of six individuals per species and transported to the field station. Here, maximum vessel lengths were estimated by cutting branches approximately 1 m from the distal apex and applying air pressure (approximately 60 kPa) (cf. Ewers and Fisher 1989) to the cut end of the branch. The distal end of the branch was then trimmed back approximately 1 cm at a time until air bubbles were seen emerging from vessel ends (Brodribb and Feild 2000). The remaining branch length at this point was then measured as an estimate of the maximum vessel length (cm).

Sapwood-specific hydraulic conductivity

A second collection of branches was made from the same six individuals per species to measure hydraulic conductivity [water flux through a unit length of stem over a pressure gradient (K_h); kg m^{-1} s^{-1} MPa^{-1}] following Sperry et al. (1988). In the field station, branches were re-cut under water to avoid the induction of new embolisms. Distal ends were trimmed with a razor blade to clear any accidentally blocked vessels and about 1 cm of the bark on each side of the branch was removed. While submerged, the shaved end of the branch was wrapped in Parafilm. All branches used for hydraulic conductivity measurements were cut to the same length (approximately 30 cm). The branch was connected to a fluid column fed by a reservoir elevated to a height of 1 m, providing a constant pressure of 9.8 kPa. An electronic balance registered KCl solution flux as an increase in sample mass every 30 s. Measurements were taken when an approximately constant flow was observed for at least 3 min. Afterwards, the stems were flushed with KCl solution at a pressure of ≈170 kPa for 10–15 min to remove emboli (Sperry et al. 1987) and hydraulic conductivity was measured again at its maximum capacity. We divided K_h by the cross-sectional area of the conductive xylem (see "Hydraulic anatomy" below), to standardize the flow of water per unit sapwood area and obtain sapwood specific hydraulic conductivity (K_s; kg m^{-1} s^{-1} MPa^{-1}). As such, hydraulic conductivity was made comparable among segments of different diameters.

Hydraulic anatomy

The same stems were then perfused with safranin dye to visualize the conductive wood area. A cross-sectional area of the upper distal end of the stem was photographed with a digital camera mounted on a microscope, at 10× magnification and the image was processed using the imaging software SigmaScan Pro 5 (SPSS) to determine vessel diameter (μm) and density (vessels mm^{-2}). For each branch, we calculated the Huber value (Hv; cm^2 cm^{-2}) as the cross-sectional sapwood area of the upper distal end of the stem divided by the total supported LA. Finally, for each species, vessel diameters were divided into 5-μm size classes to construct frequency histograms. In line with the Hagan–Poiseuille law, the vessel ratios in each size class were raised to the fourth power and summed to determine the relative contribution of each vessel size class to overall hydraulic conductance (Choat et al. 2005).

Data analysis

Differences in leaf traits (LMA, LA, g_s and A_{max}), hydraulic traits (vessel diameter and density, K_s and Hv), and traits derived from pressure–volume curves (π_0, π_{tlp}, RWC_{tlp} and ε) were contrasted among three tree species using a multivariate ANOVA (MANOVA). Because MANOVA showed significant species effects, we conducted a series of univariate ANOVAs followed by post hoc Tukey tests to identify individual responses of each trait. Overall multivariate relations and trait differences among species were further explored using a principal components analysis (PCA). Differences in traits derived from pressure–volume curves between leeward and core zones from *A. punctatum* and *M. correifolia* individuals were analyzed

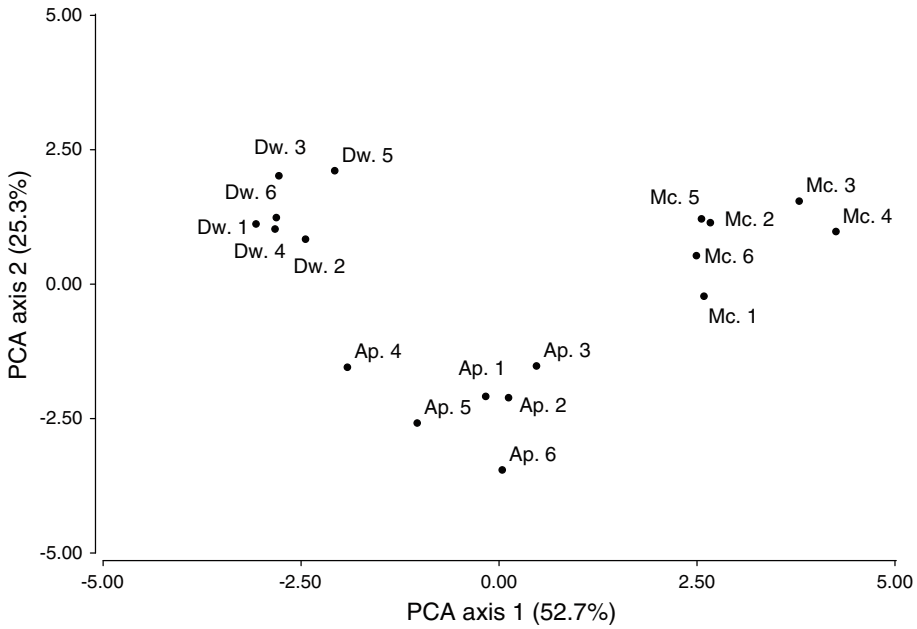

Fig. 1 Principal component analysis (PCA) of hydraulic and leaf traits of individuals of three tree species in Fray Jorge forest patches. Eigenvector scores of all traits along PCA axes are given in Table 1. *Ap Aextoxicon punctatum*, *Dw Drimys winteri*, *Mc Myrceugenia correifolia*

with independent-samples *t*-tests. Statistical analyses were performed using InfoStat (Di Rienzo et al. 2011).

Results

Species differences in leaf and hydraulic traits

Leaf and hydraulic traits, as well pressure–volume curve related traits, differed substantially among the three coexisting tree species in Fray Jorge forest (MANOVA; Wilk's = 9.9 × E−05; $F = 33.11$; $P < 0.0001$). Trait differentiation among species is best described by PCA. The first component, which explained 53 % of trait variation, showed an even contribution of variables with a magnitude of 0.3, and it clearly separated *M. correifolia* from *D. winteri*, placing *A. punctatum* at an intermediate position (Fig. 1). This component was negatively correlated with leaf traits that increased water transpiration and carbon gain (LA, g_s, A_{max}), as well as with the solute potential at full turgor (π_0) and the potential at turgor loss point (π_{tlp}) (Table 1). Then, higher values along the first PCA component reflect stronger ability to conserve water and tolerate to drought, but lower gas exchange rates. PCA component 1 was also positively correlated with vessel diameter and negatively correlated with vessel density (Table 1). The second component explained an additional 25.3 % of the total variance and it separated *A. punctatum* from the other two species. This component was dominated by higher values of RWC_{tlp} and lower values of Hv (Table 1).

Significant differences in leaf traits among species were additionally detected using separate ANOVAs (Table 2). Accordingly, we found that *D. winteri*, a tree restricted to the moist cores of large patches, exhibited a higher g_s and A_{max} than the other two species, although its average LMA did not differ from that of *A. punctatum*. In turn, we found that *M. correifolia*, a tree that occurs primarily in the drier leeward edges, had the smallest LA and lower g_s and A_{max}. Finally, the most widespread tree species in these patches, *A. punctatum,* did not differ in g_s and A_{max} from *M. correifolia* (Table 2; Fig. 2).

Clear differences among the three species in traits derived from pressure–volume curves were also found (Table 2). The two species with more sclerophyllous leaves, *A. punctatum* and *M. correifolia*, showed the lowest π_{tlp} and π_0 values, and *A. punctatum* had the lowest RWC_{tlp} (Table 2). The latter species also had the lowest ε, while values between the other two tree species did not differ.

ψ_{PD} and ψ_{MD} varied strongly among species (Table 2). In the summer season, presumably the warmer and drier period of the year, ψ_{PD} ranged from −0.075 to −0.144 MPa, while ψ_{MD} ranged from −0.28 to −0.35 MPa across the three species. ψ_{MD} never dropped below the turgor loss point, suggesting that species did not suffer from drought stress during the period of study.

We found significant differences in hydraulic traits among tree species (Table 2). Hydraulic conductivity and vessel densities were higher and vessel diameters were smaller for *D. winteri* than for the other two species (Table 2; Fig. 2). Contrary to our predictions, *M. correifolia*, the species that is most restricted to the semiarid Mediterranean-climate region, and presumably better adapted to summer drought, had larger vessel diameters than the other two species. *A. punctatum*, a

Table 1 Eigenvector scores of leaf and hydraulic traits on two main principal components analysis (*PCA*) axes

Variables	PCA 1 (52.7 %)	PCA 2 (25.3 %)
LA	−0.34	−0.06
LMA	0.34	0.21
A_{max}	−0.31	0.23
g_s	−0.32	0.23
π_0	−0.35	0.00
π_{tlp}	−0.32	0.13
RWC_{tlp}	−0.04	0.51
ε	0.22	0.42
VD	−0.35	−0.15
VDi	0.37	0.11
K_s	−0.2	0.39
Hv	−0.03	−0.45

Values *in parentheses* indicate the percentage of total variance accounted for by each axis

LA Leaf area, *LMA* leaf mass area, A_{max} photosynthetic rate, g_s stomatal conductance, π_0 solute potential at full turgor, π_{tlp} water potential at turgor loss, RWC_{tlp} relative water content at turgor loss point, ε bulk modulus of elasticity, *VD* vessel density, *VDi* vessel diameter, K_s sapwood-specific hydraulic conductivity, *Hv* Huber value

predominantly coastal tree species, with a broad latitudinal distribution in Chilean forests and in the Fray Jorge forest patch mosaic, showed the lowest hydraulic conductivity, with intermediate vessel diameters and densities (Table 2; Fig. 2). According to the Hagan–Poiseuille law, which states that in theory a vessel's hydraulic conductance is proportional to the fourth power of its radius, the hydraulic conductivities of *D. winteri* and *A. punctatum* depended strongly on the lower vessel size classes (10–20 μm), 92.7 % and 56.6 %, respectively (Fig. 3), while *M. correifolia* showed a greater range of diameter classes and had 52 % of its hydraulic conductivity accounted for by the wider vessel size class (20–30 μm) (Fig. 3).

Trait differences between patch core and leeward edge individuals

We compared traits derived from pressure–volume curves between individuals growing in the patch core (away from edges) and in the leeward edge of the same patches; this comparison was only possible for *A. punctatum* and *M. correifolia* as these species co-occur in these two microhabitats. We did not have comparative data for *D. winteri*, because it was never found in patch edges. Most physiological traits obtained from the pressure–volume curves did not differ between *A. punctatum* trees in the core and leeward trees (Table 3), except for parameter ε. In the latter case, trees on the leeward edge of patches had a lower ε than patch core trees. In contrast, *M. correifolia* showed clear differences in several attributes between trees sampled in the patch core and in the drier leeward edge. For this species, π_{tlp} and RWC_{tlp} values were lower at the leeward edge than at the patch core

Table 2 Among-species variation in leaf and hydraulic traits

	Myrceugenia correifolia	*Aextoxicon punctatum*	*Drimys winteri*	*F*	*P*
Leaf traits					
LA	6.12 ± 0.38 a	30.04 ± 3.07 b	40.20 ± 4.48 b	30.93	<0.0001
LMA	0.02 ± 0.0006 b	0.0098 ± 0.0005 a	0.0094 ± 0.0003 a	256.20	<0.0001
A_{max}	3.48 ± 0.12 a	4.34 ± 0.45 a	7.58 ± 0.47 b	31.59	<0.0001
g_s	44.08 ± 3.98 a	47.83 ± 5.41 a	77.42 ± 3.69 b	17.03	0.0001
Traits derived from pressure–volume curve					
π_0	−0.89 ± 0.05 a	−0.69 ± 0.07 b	−0.57 ± 0.03 b	11.63	0.0009
π_{tlp}	−1.18 ± 0.05 a	−1.05 ± 0.10 a	−0.81 ± 0.02 b	8.61	0.0032
RWC_{tlp}	96.51 ± 0.23 b	95.26 ± 0.23 a	96.98 ± 0.23 b	15.02	0.0003
ε	24.66 ± 1.87 b	12.13 ± 1.13 a	18.81 ± 1.83 b	14.48	0.0003
ψ_{PD}	−0.075 ± 0.01 a	−0.144 ± 0.01 b	−0.138 ± 0.012 b	25.6	<0.0001
ψ_{MD}	−0.35 ± 0.05 a	−0.32 ± 0.04 a	−0.28 ± 0.01 a	0.94	0.4127
Hydraulic traits					
VD	158.57 ± 10.41 a	294.46 ± 14.69 b	310.92 ± 9.58 b	50.43	<0.0001
VDi	21.42 ± 0.42 c	16.55 ± 0.55 b	15.01 ± 0.11 a	67.98	<0.0001
K_s	0.44 ± 0.04 a	0.38 ± 0.03 a	0.59 ± 0.02 b	11.12	0.0011
Hv	$5 \times 10^{-6} \pm 1 \times 10^{-6}$ a	$1.5 \times 10^{-5} \pm 3 \times 10^{-6}$ b	$4 \times 10^{-6} \pm 2.42 \times 10^{-7}$(a)	10.33	0.0015

Values indicate the mean ± SE for each trait per species ($n = 6$). $F_{(2,15)}$- and *P*-values from univariate ANOVA. *Different letters* represent statistical differences between species for each trait according to a post hoc Tukey test ($\alpha = 0.05$). For trait abbreviations, see Table 1

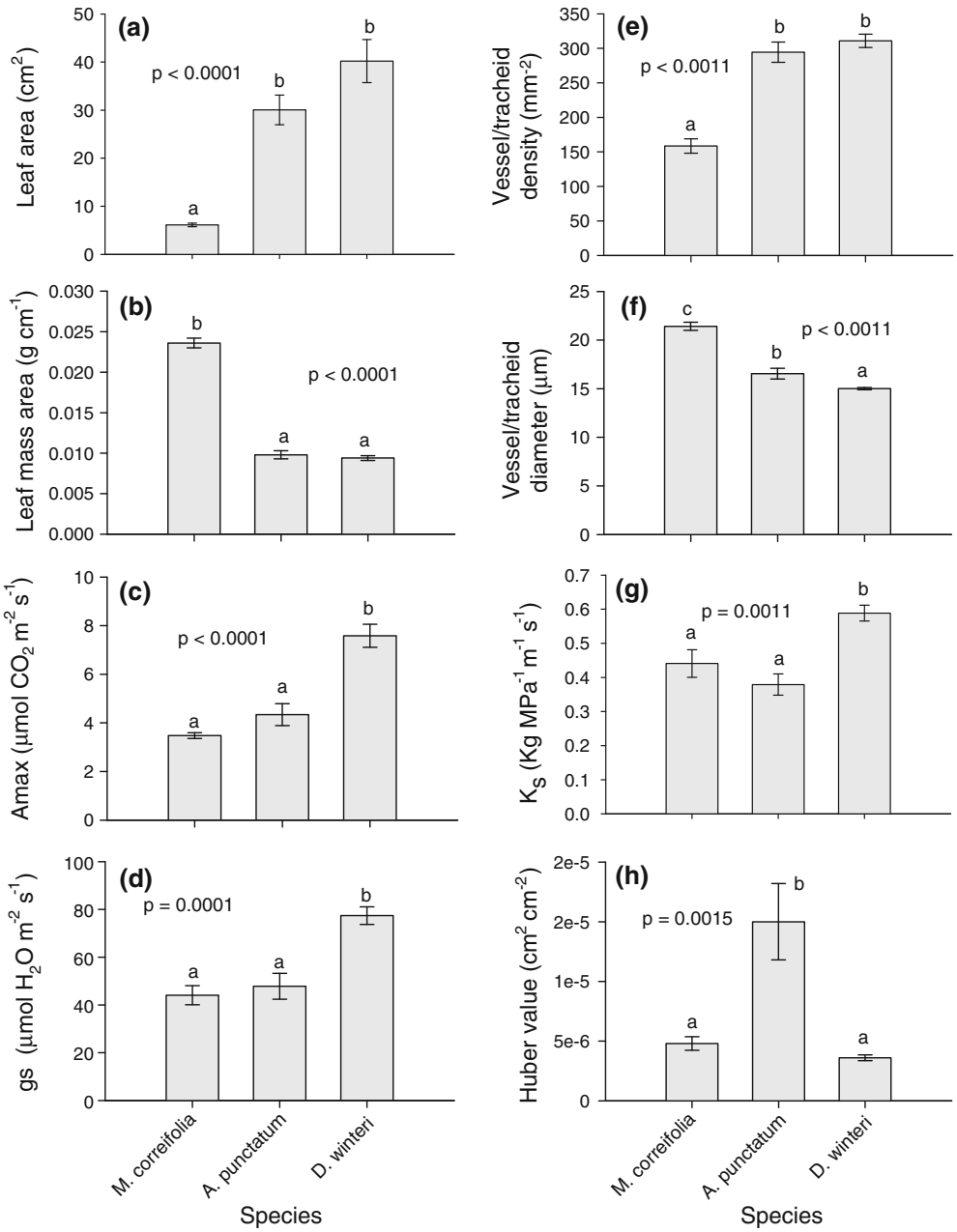

Fig. 2 Differences in leaf and hydraulic traits for three tree species in the Fray Jorge forest patches in semiarid Chile. **a** Leaf area, **b** leaf mass area, **c** photosynthetic rate (A_{max}), **d** stomatal conductance (g_s), **e** vessel/tracheid density, **f** vessel/tracheid diameter, **g** sapwood-specific hydraulic conductivity (K_s), and **h** Huber value. *Bars* represent mean ± SE. *Different letters* above the bars represent statistical differences between species for each trait resulting from univariate ANOVA with a post hoc Tukey test (see Table 2 for statistics)

(Table 3). In the case of *M. correifolia*, ε did not vary between trees in the core and leeward edge of patches. Significant differences in ψ_{PD} and ψ_{MD} between trees in patch core and those in the leeward edge were found for both species, with the lowest values found for trees at the leeward edge (Table 3). In contrast to *M. correifolia*, for *A. punctatum* trees found at the leeward edge, ψ_{MD} dropped below π_{tlp}.

Discussion

Our results indicate that evergreen tree species were able to partition small-scale, fog-dependent forest patches with strong soil moisture gradients, due to their differential ability to use soil water and tolerate drought-related habitat differences. For the three species dominating the canopy of fog-inundated patches in this semiarid region, we identified

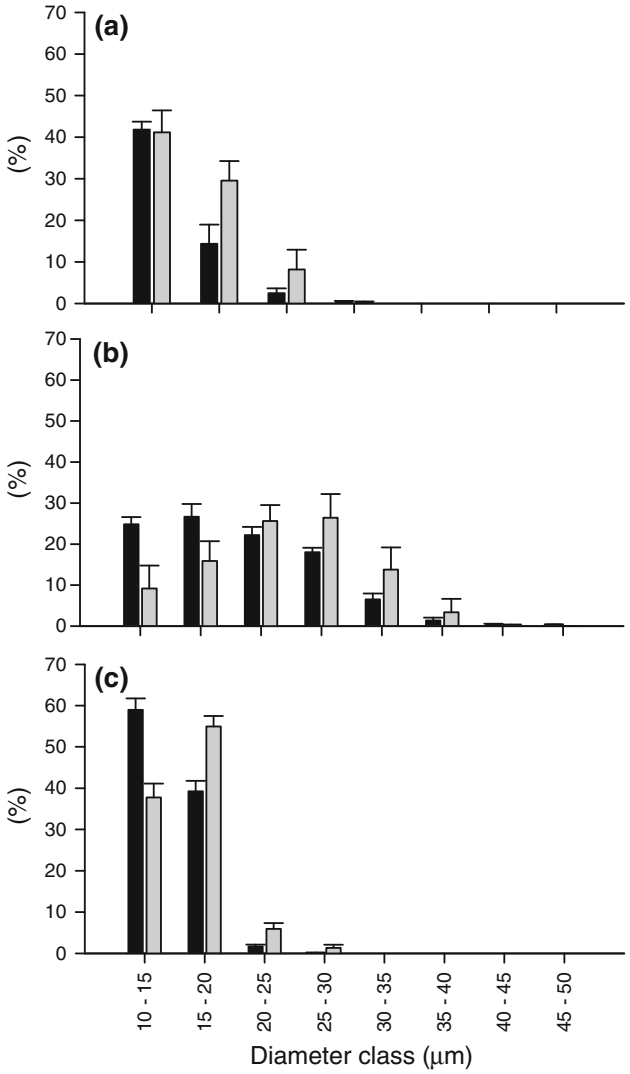

Fig. 3 Frequency distributions of xylem vessel diameters in cross-sections of branches of three tree species in Fray Jorge forest patches: **a** *A. punctatum*, **b** *M. correifolia*, **c** *D. winteri*. Plots show the number of vessels in 5-µm size classes as percentages of the total number of vessels in a given cross-sectional area (*black bars*) and the contribution of each size class to the theoretical hydraulic conductance of the branch (following the Hagan–Poiseuille Law) (*grey bars*). *Bars* represent mean values ± SE ($n = 6$)

a continuous gradient of water-use strategies. Ecophysiological strategies varied between a set of plant traits that allow efficient water transport and high carbon gain, at the one end, to traits that enhance water conservation at the cost of lower gas exchange rates, at the opposite end. At one end of the continuum we find *D. winteri*, a tree species restricted to wet microhabitats in the core of large forest patches, which has high K_s, LA, A_{max} and g_s. The opposite end of this gradient is occupied by *M. correifolia,* a species that is typically found in drier microhabitats of the leeward edges and in small forest patches, showing traits that imply increased drought tolerance, such as a small LA, reduced g_s and hydraulic conductivity, and low water potentials at turgor loss point. Finally, *A. punctatum*, the most abundant and widespread species in different microhabitats of Fray Jorge forest patches, displays intermediate values for the drought-tolerance traits investigated. The morphological and physiological differences detected among tree species in this ecosystem are likely to be important in shaping species-specific responses to future reductions in water availability as produced by reductions in fog frequency and rainfall that are predicted for this and other semiarid regions in the coming decades (Johnstone and Dawson 2010).

In this forest, *D. winteri* showed the broadest LA, highest A_{max} and greatest g_s, which are associated with the highest K_s. High conductivity contributes to a more efficient water supply to the leaves, supporting greater carbon assimilation (Meinzer et al. 1995; Sperry 2000; Brodribb and Feild 2000; Santiago et al. 2004). Still, in contrast with the former suite of traits, *D. winteri* had the smallest vessel diameters and the highest vessel density among species. *D. winteri* is an angiosperm, but belongs to the very primitive family Winteraceae, which does not have true vessels, but instead tissues that are very similar to the tracheids of coniferous species. Species with such vessel-less wood are known to have up to 21 times lower inter-element pit resistance than eudicot vessels and, therefore, their wood is highly conductive despite the short length and narrow diameter of tracheids (Hacke et al. 2006, 2007; Sperry et al. 2007). Despite its high K_s, large LA, and high g_s, *D. winteri* has a reduced ability to regulate water loss (Feild et al. 1998). Low stomatal control in *D. winteri* is probably associated with its hydrophobic granular plug, which consists of a porous, granular material that fills the stomatal cavity above the guard cells preventing them from fully closing (Feild et al. 1998; Feild and Holbrook 2000). This seems to be an adaptation to humid environments, where it precludes the formation of a permanent water film on the leaf surface that would obstruct CO_2 diffusion into the leaf (Feild et al. 1998). Consequently, a reduced ability to regulate water loss in *D. winteri* implies a greater hydraulic demand that cannot be satisfied under the drier conditions that characterize small forest patches or patch edges in Fray Jorge. Species such as *D. winteri* will be more vulnerable to increased moisture stress at patch edges, as created by fragmentation. This will be further accentuated by the regional reductions in rainfall or fog inputs and will likely reduce the possibility that this species is able to maintain a viable population in the future.

By contrast, *M. correifolia*, which is typically found in drier microhabitats in Fray Jorge, showed an opposite suite of traits compared to *D. winteri*, including smaller LAs, higher LMA, and a reduced g_s and hydraulic conductance. The combination of these traits will enhance water

Table 3 Differences in pressure–volume curve traits between individual trees growing in the patch cores (*core*) and leeward edge (*edge*) for two dominant tree species: *A. punctatum* and *M. correifolia*

Species	Traits	Core	Edge	*t*-test	*P*
A. punctatum	π_0	−0.69 ± 0.07	−0.84 ± 0.05	1.85	0.0939
	π_{tlp}	−1.05 ± 0.10	−1.18 ± 0.05	1.14	0.2805
	RWC_{tlp}	95.26 ± 0.23	95.18 ± 0.58	0.13	0.8992
	ε	12.13 ± 1.13	17.94 ± 1.17	−3.57	0.0051
	ψ_{PD}	−0.144 ± 0.01	−0.77 ± 0.05	−8.42	<0.0001
	ψ_{MD}	−0.32 ± 0.04	−1.39 ± 0.04	−10.82	<0.0001
M. correifolia	π_0	−0.89 ± 0.05	−1.15 ± 0.16	1.58	0.1658
	π_{tlp}	−1.18 ± 0.05	−1.58 ± 0.15	2.47	0.0487
	RWC_{tlp}	96.51 ± 0.23	95.51 ± 0.23	3.12	0.0108
	ε	24.66 ± 1.87	24.51 ± 3.05	0.04	0.9673
	ψ_{PD}	−0.075 ± 0.01	−0.32 ± 0.02	−14.44	<0.0001
	ψ_{MD}	−0.35 ± 0.05	−0.97 ± 0.05	−5.39	0.0007

$t_{(10)}$- and *P*-values result from *t*-tests. For trait abbreviations, see Table 1

conservation under water stress, but have a cost on gas exchange rates. A_{max} measured in the field in *M. correifolia* was two times lower than in the less-stress tolerant *D. winteri*. *M. correifolia* also showed a greater range of vessel diameter classes than the other two species, implying greater functional diversity for this trait. Wider vessels are more efficient in water transport and could be useful in wetter habitats and wetter periods of the year, while in the drier season or drier habitats, when wider vessels are more prone to cavitation, *M. correifolia* can use its narrower vessels to maintain water transport. The wider range of vessel sizes exhibited by *M. correifolia* likely explains the ability of this species to cope with the strong fluctuations in water availability that characterize small patches and leeward edges (Barbosa et al. 2010), where it is found. Accordingly, among the three species studied, *M. correifolia* is the most capable of tolerating a substantial increment of climatic variability and more extreme droughts, as expected from global climate change in this region. *M. correifolia* is thus most likely to profit from the altered climate conditions as expected for this region.

Finally, *A. punctatum*, the most abundant and widespread species in Fray Jorge forest patches, had similar levels of stomatal and hydraulic conductance and A_{max} as *M. correifolia*, even though *A. punctatum* is a temperate tree species with sclerophyllous leaves that generally occurs in areas of higher rainfall at higher latitudes in south-central Chile. We suggest that the unexpectedly low values of π_{tlp} recorded in this species could be a response to the strong effects of oceanic salt spray over most of its coastal distribution (Pérez and Villagrán 1985), which is intercepted by the crown foliage and branches, and conducted to the soil via throughfall and stemflow (Ponette-González et al. 2009). The high salt content of marine spray and rain water in Chilean coastal forests (Hedin et al. 1995) can reduce soil osmotic potential and thus soil water potential, forcing tree species to limit ψ as a mechanism to sustain soil water absorption and transport. Individuals of *A. punctatum* growing in the forest patch core have lower ψ_{PD} values than the more drought-tolerant *M. correifolia*, which may have deeper root systems, which allows a better access to deeper soil water reserves. This could also explain why this species showed a greater capacity to rehydrate overnight than the other two evergreen tree species in Fray Jorge.

Despite interspecific differences in ψ_{PD} and ψ_{MD}, all three species showed ψ_{MD} values higher than π_{tlp} when growing in the forest patch core, confirming that frequent summer fog in Fray Jorge represents an effective physical buffer against diurnal temperature fluctuations and desiccation that characterize the semiarid surrounding vegetation (del-Val et al. 2006; Ewing et al. 2009). Trees of *M. correifolia* and *A. punctatum* occurring at the leeward edge of Fray Jorge forest patches had lower ψ_{PD} values than those trees occurring in the patch core, showing that trees along edges have more limited access to soil moisture and lower capacity to rehydrate and recover leaf water status overnight. For the more drought-resistant *M. correifolia,* ψ_{MD} values were higher than π_{tlp} values, but in the case of *A. punctatum* they were lower. These results indicate that in leeward patch edges, *A. punctatum*, but not *M. correifolia*, experiences more water stress, and therefore it might be unable to recover its leaf water status overnight, after losing substantial water by transpiration during the day. Interspecific differences can be best explained by pressure–volume curves. Trees of *M. correifolia* in the leeward edge had the most negative osmotic potentials at full turgor and at turgor loss point, and lower cell water content at turgor loss point than trees of the same species in the patch core. In turn, the ε did not vary between habitats. According to these results, *M. correifolia* appears to be able to tolerate (rather than avoid) drought (Bartlett et al. 2012) by adjusting its osmotic potential at cell level, as reflected in a reduced π_0. Such compensatory osmotic mechanisms have

been described in south-central Chile for the trees *Kageneckia oblonga* (Cabrera 2002) and *Eucryphia cordifolia* (Figueroa et al. 2010). In contrast to *M. correifolia*, *A. punctatum* did not show much variation in pressure–volume parameters between trees in patch core habitats and leeward edges, except for ε, resulting in ψ_{MD} values which were lower than π_{tlp} values, and therefore, significant water stress at leeward edges. This suggests that over longer time periods, increased water stress can result in a negative water balance for *A. punctatum* trees that occur in the leeward edge of patches. This might also explain the increased mortality rates and lower regeneration of *A. punctatum* observed in leeward edges compared to windward edges and patch cores (del-Val et al. 2006). Considering that global change scenarios for this region of the world predict increased patch fragmentation (Sala et al. 2000), and therefore enhanced edge effects in forested landscapes, *A. punctatum* trees will be at increased risk of mortality due to drought conditions along patch edges. In Fray Jorge, the disruption of the canopy of *A. punctatum* in forest patches, due to enhanced drought or lower fog inputs, may substantially reduce the fog interception capacity of patches. In turn, this could modify the hydrological balance of the forest and affect the regeneration and persistence of other tree species that depend on the fog capture by the *A. punctatum* canopy (Gutiérrez et al. 2008).

Overall, our findings support the broader concept that along pronounced soil moisture gradients driven by fog interception in forest patches, tree functional diversity is strongly linked to interspecific differences in drought tolerance and/or efficiency of water use. We emphasize that plant hydraulic traits play a fundamental role in explaining niche differentiation among species in patch center-to-edge habitats and their quantitative understanding is key to predicting how forests will respond to future scenarios of land use and climate change.

Acknowledgments We would like to express our gratitude to Leonardo Ramirez, Felipe Albornoz, Rafaella Canessa, Aurora Gaxiola, Paulina Lobos, Juan Monardez, Carmen Ossa, Daniel Salinas, Daniel Stanton and Patricio Valenzuela for their invaluable assistance in the field and useful discussions and comments on the manuscript. This work was supported by CONICYT fellowship 24110074 to B. S.-N., and grants Fondecyt 1110929 to F. P., P05-002 from Millennium Scientific Initiative and PFB-23 from CONICYT to the Institute of Ecology and Biodiversity, Chile. This study is a contribution to LINC-Global (Chile-Spain) and to the Research Program of the Chilean Long-Term Socio-Ecological Research network at Fray Jorge National Park.

References

Baltzer JL, Davies SJ, Bunyavejchewin S, Noor NSM (2008) The role of desiccation tolerance in determining tree species distributions along the Malay–Thai Peninsula. Funct Ecol 22:221–231. doi:10.1111/j.1365-2435.2007.01374.x

Barbosa O, Marquet PA, Bacigalupe LD, Christie DA, del-Val E, Gutiérrez AG, Jones CG, Weathers KC, Armesto JJ (2010) Interactions among patch area, forest structure and water fluxes in a fog-inundated forest ecosystem in semi-arid Chile. Funct Ecol 24:909–917. doi:10.1111/j.1365-2435.2010.01697.x

Bartlett M, Scoffoni C, Sack L (2012) The determinants of leaf turgor loss point and prediction of drought tolerance of species and biomes: a global meta-analysis. Ecol Lett 15:393–405. doi:10.1111/j.1461-0248.2012.01751.x

Bongers F, Poorter L, Van Rompaey RSAR, Parren MPE (1999) Distribution of twelve moist forest canopy tree species in Liberia and Cote d'Ivoire: response curves to a climatic gradient. J Veg Sci 10:371–382. doi:10.2307/3237066

Brodribb TJ, Feild TS (2000) Stem hydraulic supply is linked to leaf photosynthetic capacity: evidence from New Caledonian and Tasmanian rainforests. Plant Cell Environ 23:1381–1388. doi:10.1046/j.1365-3040.2000.00647.x

Cabrera HM (2002) Ecophysiological responses of plants in ecosystems with Mediterranean-like climate and high mountain environments. Rev Chil Hist Nat 75:625–637

Cereceda P, Osses P, Larraín H, Farías M, Lagos M, Pinto R, Schemenauer RS (2002) Advective, orographic and radiation fog in the Tarapacá region, Chile. Atmos Res 64:261–271

Choat B, Marilyn CB, Luly JG, Holtum JAM (2005) Hydraulic architecture of deciduous and evergreen dry rainforest tree species from north-eastern Australia. Trees Struct Funct 19:305–311. doi:10.1007/s00468-004-0392-1

Condit R (1998) Ecological implications of changes in drought patterns: shift in forest composition in Panama. Clim Change 39:413–427. doi:10.1023/A:1005395806800

Condit R, Pitman N, Leigh EG Jr, Chave J, Terborgh J, Foster RB, Nuñez-V P, Aguilar S, Valencia R, Villa G, Muller-Landau HC, Losos E, Hubbell SP (2002) Beta-diversity in tropical forest trees. Science 295:666–669. doi:10.1126/science.1066854

Cornelissen JHC, Lavorel S, Garnier E, Díaz S, Buchmann N, Gurvich DE, Reich PB, ter Steege H, Morgan HD, van der Heijden MGA, Pausas JG, Poorter H (2003) A handbook of protocols for standardised and easy measurement of plant functional traits worldwide. Aust J Bot 51:335–380. doi:10.1071/BT02124

Dawson TE (1998) Fog in the California redwood forest: ecosystem inputs and use by plants. Oecologia 117:476–485. doi:10.1007/s004420050683

del-Val E, Armesto JJ, Barbosa O, Christie DA, Gutiérrez AG, Jones CG, Marquet PA, Weathers KC (2006) Rain forest islands in the Chilean semiarid region: fog-dependency, ecosystem persistence and tree regeneration. Ecosystems 9:598–608. doi:10.1007/s10021-006-0065-6

Di Castri F, Hajek E (1976) Bioclimatología de Chile. Universidad Católica de Chile, Santiago

Di Rienzo JA, Casanoves F, Balzarini MG, Gonzalez L, Tablada M, Robledo CW (2011) InfoStat versión 2011. Grupo InfoStat, FCA, Universidad Nacional de Córdoba, Argentina. http://www.infostat.com.ar

Engelbrecht BMJ, Comita LS, Condit R, Kursar TA, Tyree MT, Turner BL, Hubbell SP (2007) Drought sensitivity shapes species distribution patterns in tropical forests. Nature 447:80–83. doi:10.1038/nature05747

Ewers FW, Fisher JB (1989) Techniques for measuring vessel lengths and diameters in 17 stems of woody plants. Am J Bot 76:645–656

Ewing HA, Weathers KC, Templer PH, Dawson TE, Firestone MK, Elliott AM, Boukili VKS (2009) Fog water and ecosystem function: heterogeneity in a California redwood forest. Ecosystems 12:417–433. doi:10.1007/s10021-009-9232-x

Feild TS, Holbrook NM (2000) Xylem sap flow and stem hydraulics of the vesselless angiosperm *Drimys granadensis* (Winteraceae) in a Costa Rican elfin forest. Plant Cell Environ 23:1067–1077. doi:10.1046/j.1365-3040.2000.00626.x

Feild TS, Zwieniecki MA, Donoghue MJ, Holbrook NM (1998) Stomatal plugs of *Drimys winteri* (Winteraceae) project leaves from mist but not drought. Proc Natl Acad Sci USA 95:14256–14259. doi:10.1073/pnas.95.24.14256

Figueroa JA, Cabrera HM, Queirolo C, Hinojosa LF (2010) Variability of water relations and photosynthesis in *Eucryphia cordifolia* Cav. (Cunoniaceae) over the range of its latitudinal and altitudinal distribution in Chile. Tree Physiol 30:574–585. doi:10.1093/treephys/tpq016

Gentry AH (1988) Changes in plant community diversity and floristic composition on environmental and geographic gradients. Ann Mo Bot Gard 75:1–34

Gutiérrez AG, Barbosa O, Christie DA, del-Val E, Ewing HA, Jones CG, Marquet PA, Weathers KC, Armesto JJ (2008) Regeneration patterns and persistence of the fog dependent Fray Jorge forest in semiarid Chile during the past two centuries. Glob Change Biol 14:161–176. doi:10.1111/j.1365-2486.2007.01482.x

Hacke UG, Sperry JS, Pockman WT, Davis SD, McCulloh K (2001) Trends in wood density and structure are linked to prevention of xylem implosion by negative pressure. Oecologia 126:457–461. doi:10.1007/s004420100628

Hacke UG, Sperry JS, Wheeler JK, Castro L (2006) Scaling of angiosperm xylem structure with safety and efficiency. Tree Physiol 26:689–701. doi:10.1093/treephys/26.6.689

Hacke UG, Sperry JS, Feild TS, Sano Y, Sikkema EH, Pittermann J (2007) Water transport in vesselless angiosperms: conducting efficiency and cavitation safety. Int J Plant Sci 168:1113–1126. doi:10.1086/520724

Hedin LO, Armesto JJ, Johnson AH (1995) Patterns of nutrient loss from unpolluted, old-growth temperate forests: evaluation of biogeochemical theory. Ecology 76:493–509

Hildebrandt A, Eltahir EAB (2006) Forest on the edge: seasonal cloud forest in Oman creates its own ecological niche. Geophys Res Lett 33:L11401. doi:10.1029/2006GL026022

Johnstone JA, Dawson TE (2010) Climatic context and ecological implications of summer fog decline in the coast redwood region. Proc Natl Acad Sci USA 107:4533–4538. doi:10.1073/pnas.0915062107

Katata G, Nagai H, Kajino M, Ueda H, Hozumi Y (2010) Numerical study of fog deposition on vegetation for atmosphere–land interactions in semi-arid and arid regions. Agric For Meteorol 150:340–353

Kozlowski TT, Pallardy SG (2002) Acclimation and adaptive responses of woody plants to environmental stresses. Bot Rev 68:270–334. doi:10.1663/0006-8101

Kursar TA, Engelbrecht BMJ, Burke A, Tyree MT, Omari BE, Giraldo JP (2009) Tolerance to low leaf water status of tropical tree seedlings is related to drought performance and distribution. Funct Ecol 23:93–102. doi:10.1111/j.1365-2435.2008.01483.x

López-Cortés F, López D (2004) Antecedentes bioclimáticos del Parque Nacional Bosque Fray Jorge. In: Squeo FA, Gutiérrez JR, Hernández IR (eds) Historia natural del parque nacional bosque Fray Jorge. Ediciones Universidad de La Serena, Chile, pp 45–60

Markesteijn L, Poorter L, Bongers F, Paz H, Sack L (2011a) Hydraulics and life history of tropical dry forest tree species: coordination of species' drought and shade tolerance. New Phytol 191:480–495. doi:10.1111/j.1469-8137.2011.03708.x

Markesteijn L, Poorter L, Paz H, Sack L, Bongers F (2011b) Ecological differentiation in xylem cavitation resistance is associated with stem and leaf structural traits. Plant Cell Environ 34:137–148. doi:10.1111/j.1365-3040.2010.02231.x

Meinzer FC, Goldstein G, Jackson P, Holbrook NM, Gutiérrez MV, Cavelier J (1995) Environmental and physiological regulation of transpiration in tropical forest gap species: the influence of boundary layer and hydraulic properties. Oecologia 101:514–522. doi:10.1007/BF00329432

Mitchell PJ, Veneklaas EJ, Lambers H, Burguess SSO (2008) Using multiple trait associations to define hydraulic functional types in plant communities of south-western Australia. Oecologia 158:385–397. doi:10.1007/s00442-008-1152-5

Pérez C, Villagrán C (1985) Distribution of species abundances in relict forests of the Mediterranean zone of Chile. Rev Chil Hist Nat 58:157–170

Ponette-González A, Weathers KC, Curran LM (2009) Water inputs across a tropical montane landscape in Veracruz, Mexico: synergistic effects of land cover, rain and fog seasonality, and interannual precipitation variability. Glob Change Biol 16:46–49. doi:10.1111/j.1365-2486.2009.01985.x

Poorter L (2007) Are species adapted to their regeneration niche, adult niche, or both? Am Nat 169:433–442

Pyke CR, Condit R, Aguilar S, Lao S (2001) Floristic composition across a climatic gradient in a neotropical lowland forest. J Veg Sci 12:553–566. doi:10.2307/3237007

Sala OE, Chapin FS III, Armesto JJ, Berlow E, Bloomfield J, Dirzo R, Huber-Sanwald E, Huenneke LF, Jackson RB, Kinzig A, Leemans R, Lodge DM, Mooney HA, Oesterheld M, Poff NL, Sykes MT, Walker BH, Walker M, Wall DH (2000) Global biodiversity scenarios for the year 2100. Science 287:1770–1774. doi:10.1126/science.287.5459.1770

Santiago LS, Goldstein G, Meinzer FC, Fisher JB, Machado K, Woodruff D, Jones T (2004) Leaf photosynthetic traits scale with hydraulic conductivity and wood density in Panamanian forest canopy trees. Oecologia 140:543–550. doi:10.1007/s00442-004-1624-1

Sperry JS (2000) Hydraulic constraints on plant gas exchange. Agric For Meteorol 104:13–23

Sperry JS, Holbrook MN, Zimmermann M, Tyree MT (1987) Spring filling of xylem vessels in wild grapevine. Plant Physiol 83:414–417

Sperry JS, Donnelly JR, Tyree MT (1988) A method for measuring hydraulic conductivity and embolism in xylem. Plant Cell Environ 11:35–40. doi:10.1111/j.1365-3040.1988.tb01774.x

Sperry JS, Hacke UG, Feild TS, Sano Y, Sikkema EH (2007) Hydraulic consequences of vessel evolution in angiosperms. Int J Plant Sci 168:1127–1139. doi:10.1086/520726

Sterck F, Markesteijn L, Schieving F, Poorter L (2011) Functional traits determine trade-offs and niches in a tropical forest community. Proc Natl Acad Sci USA 108:20627–20632. doi:10.1073/pnas.1106950108

Villagrán C, Armesto JJ, Hinojosa LF, Cuvertino J, Pérez C, Medina C (2004) El enigmático origen del bosque relicto de Fray Jorge. In: Squeo FA, Gutiérrez JR, Hernández IR (eds) Historia natural del parque nacional bosque Fray Jorge. Ediciones Universidad de La Serena, Chile, pp 3–43

Weathers KC, Lovett GM, Likens GE, Caraco NFM (2000) Cloud-water inputs of nitrogen to forest ecosystems in southern Chile: forms, fluxes and sources. Ecosystems 3:590–595. doi:10.1007/s100210000051

Wright SJ (1992) Seasonal drought, soil fertility and the species density of tropical forest plant communities. Trends Ecol Evol 7:260–263